

SO₂ over central China: Measurements, numerical simulations and the tropospheric sulfur budget

Hao He,¹ Can Li,^{2,3} Christopher P. Loughner,^{2,3} Zhanqing Li,^{1,3,4} Nickolay A. Krotkov,² Kai Yang,^{1,2} Lei Wang,⁵ Youfei Zheng,⁵ Xiangdong Bao,⁶ Guoqiang Zhao,⁶ and Russell R. Dickerson^{1,3,7}

Received 28 June 2011; revised 4 December 2011; accepted 5 December 2011; published 9 February 2012.

[1] SO₂ in central China was measured in situ from an aircraft and remotely using the Ozone Monitoring Instrument (OMI) from the Aura satellite; results were used to develop a numerical tool for evaluating the tropospheric sulfur budget - sources, sinks, transformation and transport. In April 2008, measured ambient SO₂ concentrations decreased from ~7 ppbv near the surface to ~1 ppbv at 1800 m altitude (an effective scale height of ~800 m), but distinct SO₂ plumes were observed between 1800 and 4500 m, the aircraft's ceiling. These free tropospheric plumes play a major role in the export of SO₂ and in the accuracy of OMI retrievals. The mean SO₂ column contents from aircraft measurements (0.73 DU, Dobson Units) and operational OMI SO₂ products (0.63 ± 0.26 DU) were close. The OMI retrievals were well correlated with in situ measurements (r = 0.84), but showed low bias (slope = 0.54). A new OMI retrieval algorithm was tested and showed improved agreement and bias (r = 0.87, slope = 0.86). The Community Multiscale Air Quality (CMAQ) model was used to simulate sulfur chemistry, exhibiting reasonable agreement (r = 0.62, slope = 1.33) with in situ SO₂ columns. The mean CMAQ SO₂ loading over central and eastern China was 54 kT, ~30% more than the estimate from OMI SO₂ products, 42 kT. These numerical simulations, constrained by observations, indicate that ~50% (35 to 61%) of the anthropogenic sulfur emissions were transported downwind, and the overall lifetime of tropospheric SO₂ was 38 ± 7 h.

Citation: He, H., et al. (2012), SO₂ over central China: Measurements, numerical simulations and the tropospheric sulfur budget, *J. Geophys. Res.*, 117, D00K37, doi:10.1029/2011JD016473.

1. Introduction

[2] Driven by the rapid economic development in the past decades, the consumption of energy and raw material in China increased dramatically. Coal burning accounts for 70% of the total energy consumption in China [CESY, 2005], and estimated total anthropogenic sulfur dioxide (SO₂) emissions were ~31.3 Tg in 2008 [Lu et al., 2010]. Atmospheric SO₂ is oxidized to form sulfate (SO₄²⁻) aerosols and leads to acid deposition through sulfuric acid (H₂SO₄). The sulfate aerosols can exert influence on weather and climate [Intergovernmental Panel on Climate Change, 2007;

Stier et al., 2007], cause visibility impairments [Hand and Malm, 2007], and pose a hazard to public health [U.S. Environmental Protection Agency, 2004; He et al., 2002; Hu et al., 2010; Kan et al., 2010; Schlesinger and Cassee, 2003]. These sulfur-compounds can be transported far from the source regions [Dunlea et al., 2009; Prospero et al., 2003; Singh et al., 2009; van Donkelaar et al., 2008].

[3] A number of studies have been conducted to investigate the sulfurous pollution in China. Surface observations of SO₂ were made in and near Beijing [C. Li et al., 2007; Sun et al., 2009], Yangtze River Delta (YRD) [Costabile et al., 2006], Pearl River Delta (PRD) [Zhang et al., 2008], and rural areas [Meng et al., 2010]. Aircraft measurements were also performed to study the vertical distribution of SO₂ in the Northeast [Dickerson et al., 2007], South [Wang et al., 2008], and East of China [Geng et al., 2009; Xue et al., 2010]. Both surface and airborne measurements demonstrated high SO₂ concentrations with large variations in spatial and temporal distributions. For instance, ambient SO₂ measurements in ten background and rural sites revealed concentrations (± standard deviation, σ) of 0.7 ± 0.4 ppbv at Waliguan on Qinghai Plateau and 67.3 ± 31.1 ppbv at Kaili in Southwest China [Meng et al., 2010]; over the PRD, investigators observed 18.5 ppbv SO₂ at 2100 m and up to 107.5 ppbv SO₂ within the planetary boundary layer (PBL)

¹Department of Atmospheric and Oceanic Science, University of Maryland, College Park, Maryland, USA.

²NASA Goddard Space Flight Center, Greenbelt, Maryland, USA.

³Earth System Science Interdisciplinary Center, University of Maryland, College Park, Maryland, USA.

⁴State Key Laboratory of Earth Surface Processes and Resource Ecology, GCESS, Beijing Normal University, Beijing, China.

⁵Nanjing University of Information Science and Technology, Nanjing, China.

⁶Henan Meteorological Bureau, Zhengzhou, China.

⁷Department of Chemistry and Biochemistry, University of Maryland, College Park, Maryland, USA.



Figure 1. Location of Henan province and Y-7 research airplane used for air sampling.

during one research flight [Wang *et al.*, 2008]; over north-eastern China 5 ~ 20 ppbv SO₂ in the PBL and <1 ppbv SO₂ aloft were observed [Dickerson *et al.*, 2007].

[4] Remote sensing of tropospheric SO₂ over China using the OMI instrument has been used to track an individual SO₂ plume [Krotkov *et al.*, 2008; Li *et al.*, 2010a] and to identify changes in emission sources [Li *et al.*, 2010b; Witte *et al.*, 2009]. OMI SO₂ products showed reasonable agreement with the in situ measurements and estimated SO₂ emission reductions based on a bottom-up approach. Numerical regional air quality models, such as the USEPA CMAQ model, have been employed to simulate the SO₂ chemistry and transport in East Asia [Lin *et al.*, 2008; Liu *et al.*, 2010; Wang *et al.*, 2010a, 2010b]. However, most of the studies focused on the highly industrialized regions of eastern China, and it is crucial to also investigate SO₂ pollution and chemistry in the developing areas of central and western China.

[5] The majority of tropospheric SO₂ is removed by dry deposition or oxidization to form sulfate aerosols (SO₄²⁻). The SO₂ dry deposition velocity has been measured at 0.2 ~ 0.4 cm/s in northern China [Clarke *et al.*, 1997; Sorimachi *et al.*, 2003; Sorimachi and Sakamoto, 2007; Wesely and Hicks, 2000]. In the PBL, the lifetime of SO₂ is a few days due to dry deposition alone [Berglen *et al.*, 2004; Chin *et al.*, 1996], and the observed lifetime is greatly decreased by oxidation processes. When lifted to the free troposphere (FT, higher than 2000 m), the atmospheric SO₂ has a longer lifetime, and the long-range transport of atmospheric SO₂ from China becomes important [Igarashi *et al.*, 2006; Kim *et al.*, 2001; Tu *et al.*, 2004]. In the U.S., it was estimated that ~30% of the emitted SO₂ is subsequently removed through dry deposition and ~37% is exported [Shannon and Sisterson, 1992]. During transport, the reactive SO₂ is oxidized to form sulfate aerosols and other sulfurous compounds [Calvert *et al.*, 1978; Cox and Penkett, 1971; Eggleton and Cox, 1978; Lee *et al.*, 2011]. Sulfate aerosols impact the global radiative balance through direct effects [Haywood and Boucher, 2000; Stier *et al.*, 2007] and indirect effects on clouds [Albrecht, 1989; Twomey, 1977]. Therefore, a budget analysis including the long-range transport and evolution of tropospheric SO₂ is essential to investigate regional air quality and large-scale climate effects.

[6] In April 2008, a joint China-U.S. field experiment was carried out under the East Asian Study of Tropospheric Aerosols and their Impact on Regional Climate (EAST-AIRC) [Li *et al.*, 2011], following the East Asian Study of Tropospheric Aerosols, an International Regional Experiment (EAST-AIRE) [Z. Q. Li *et al.*, 2007]. In addition to ground-based campaigns at four locations in southern and northern

China, an airborne campaign on ambient SO₂ was conducted in Henan province, central China (Figure 1). Coalmines and power plants are concentrated in western and southern Henan, and coal burning is ubiquitous for domestic cooking and heating. In 2007, Henan emitted 2.3 Tg SO₂, around 7% of the total emission of China, and the power plants emissions were 1.1 Tg SO₂, ranking 3rd in China by province [Lu *et al.*, 2010]. Central China is a major source of sulfur emissions that has not been thoroughly investigated.

[7] In this article, we present a study of tropospheric sulfurous pollutants over central China, employing in situ measurements (aircraft campaign), satellite remote sensing (NASA OMI SO₂ products), and numerical simulations (the CMAQ system). Section 2 presents the data set and methods applied. Section 3 describes results from aircraft measurements of tropospheric SO₂. In section 4, we compare OMI SO₂ products with in situ measurements. Section 5 describes the set-up of CMAQ system, management of emission inventory, and model modification. In section 6 we discuss the CMAQ results, model evaluation, SO₂ lifetime and transport of sulfur-compounds. Finally we summarize the in situ observations, remotely sensed observations and numerical simulations to estimate the fraction of sulfur emitted into the atmosphere then exported from central China to the atmosphere over the Pacific.

2. Data and Method

[8] For the aircraft campaign, a Y-7 turboprop transport aircraft (the Chinese version of Antonov An-26, Figure 1) was employed as the measurement platform. This airplane with a cruise speed of 400 km/h was based at the Xinzheng International Airport (IATA code: CGO, 34.52°N, 113.84°E) in suburban Zhengzhou, the capitol city of Henan with 7 million residents. The aft-facing inlet and the temperature/relative humidity (T/RH) probe provided by the local Henan Meteorological Bureau (HMB) were installed on a rack to the left of fuselage. HMB also provided GPS and other logistical support.

[9] A commercially available Thermo Electron Corporation (TECO) 43C trace level pulsed fluorescence SO₂ analyzer was modified to measure the ambient SO₂ [Luke, 1997], with a detection limit enhanced to ~0.3 ppbv for 10 s averaging time [Hains, 2007]. The instrument was calibrated with a National Institute of Standard and Technology (NIST) traceable SO₂ gas standard (Scott Marrin INC., Riverside CA, U.S.A.). HMB provided 1 s data of altitude, longitude, latitude, ambient temperature (T) and relative humidity (RH), which were processed to 10 s average data and checked for quality assurance.

[10] Flight routes were selected based on the near real-time OMI SO₂ maps (http://so2.gsfc.nasa.gov/pix/daily/0408/china_0408z.html) provided by the NASA OMI SO₂ group. Synoptic circulation patterns were tracked through satellite images, surface analyses and forecasts (<http://web.kma.go.kr/eng/index.jsp>) from the Korea Meteorological Administration (KMA). Flight plans were designed to measure ambient SO₂ over locations with both strong and weak OMI SO₂ signals under different weather conditions. We took off around 1 P.M. local time (0500 UTC), so the spirals were conducted between 1 and 2 P.M. local time, close to the OMI overpass time (1:45 P.M.). The research flights

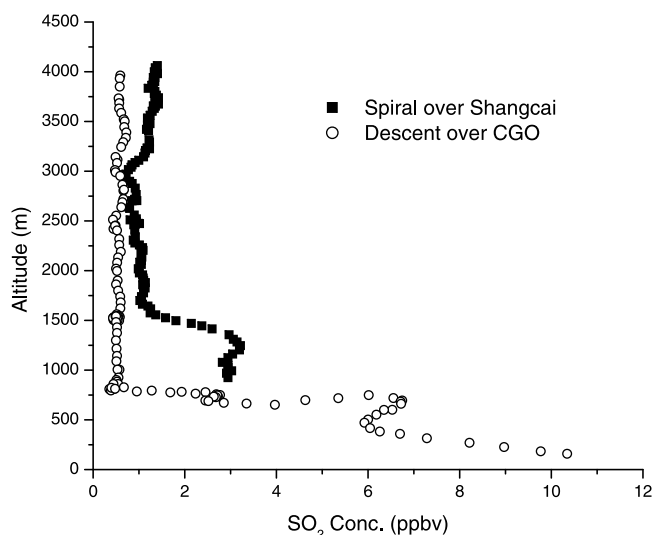


Figure 2. SO₂ Altitude profiles from research flight 04/15/2008. Shangcai (33.25°N, 114.26°E) was a moderate OMI SO₂ signal region, and the descent was over CGO airport (34.52°N, 113.84°E).

were confined within the province, and the spirals were restricted to altitudes of 900 ~ 4500 m for safety concerns. We retrieved the information of SO₂ within the PBL (lower than 1000 m, a typical PBL height during spring in China) during the descents into the airport.

[11] The backscattered UV radiation measurements from OMI were used to retrieve SO₂ PBL column amounts through the operational Band Residual Difference (BRD) algorithm [Krotkov *et al.*, 2006]. This algorithm was validated over Northeastern China during the EAST-AIRE campaign [Krotkov *et al.*, 2008] and utilized to create operational products. Daily OMI SO₂ and cloud composite images were available from the NASA SO₂ web site (<http://so2.gsfc.nasa.gov>). In this study, we applied the OMI daily gridded products (SO2L2G, hereafter named OMISO2 products, available at http://disc.sci.gsfc.nasa.gov/Aura/data-holdings/OMI/OMISO2g_v003.shtml). These daily products were filtered to remove data with high radiative cloud fraction (OMI cloud fraction >0.3) and large solar zenith angle (SZA > 70°).

[12] In an effort to improve the detection and quantification of SO₂ from OMI, we have also utilized an advanced retrieval technique, the iterative spectral fitting (ISF) algorithm, previously applied to volcanic clouds [Yang *et al.*, 2009a, 2009b, 2010], to take advantage of the large number of spectral measurements available from the hyperspectral instruments, such as OMI and GOME-2. The ISF algorithm provides less noisy and potentially more accurate column estimates under the diverse range of conditions encountered in global observations, and has been extended to extract the height of a volcanic SO₂ layer in the atmosphere [Yang *et al.*, 2009a, 2010]. The ISF products were generated deliberately off-line for 2008 campaign over the East Asia area.

[13] We applied the WRF (Weather Research and Forecasting) - MCIP (Meteorology-Chemistry Interface Processor) - CMAQ system to conduct numerical simulations for our campaign. NASA 2006 Intercontinental Chemical

Transport Experiment Phase-B (INTEX-B) emission inventory [Zhang *et al.*, 2009] was utilized to create emission input data for CMAQ. MCIP was developed to correct SO₂ dry deposition velocity, and CMAQ was modified to calculate the flux of pollutants entering and exiting the modeling domain. Hourly outputs of CMAQ simulations were stored and analyzed. Details on the model system are described in section 5.

3. Results of Aircraft Campaign

[14] During the month-long aircraft campaign for cloud-seeding operations, seven research flights were conducted on April 4, 5, 15, 16, 18, 20, and 22, 2008. These flights were within 150 km of the CGO airport, covering regions with strong OMI SO₂ signal such as Changyuan (34.52°N, 113.85°E) and those with weak OMI SO₂ signal such as Yexian (33.62°N, 113.35°E). Figure 2 shows the SO₂ profiles observed on 04/15/2008. The destination, Shangcai (33.25°N, 114.26°) had a moderate OMI SO₂ pollution, and relatively high SO₂ concentration (up to 1.5 ppbv) was observed at high altitudes, ~4000 m. Table 1 presents a statistical analysis of ambient SO₂ concentrations averaged in 500 m layers from the surface to 4000 m. Over Changyuan (April 4th and 5th), we observed up to 7 ppbv SO₂ at 2000 m, while over Yexian (April 18th and 22nd) the ambient SO₂ concentration was below the detection limit (~0.3 ppbv). The results were consistent with the OMI SO₂ maps. During the descents over the CGO airport, relatively high concentrations of SO₂ were observed consistently, pointing to the urban area of Zhengzhou as a stationary source of the SO₂ pollution. High concentrations of SO₂ were found below ~500 m altitude, implying that the substantial amount of ambient SO₂ was concentrated within the PBL.

[15] A summary of flight routes (auxiliary material Figure S1) shows a relatively homogeneous sampling over the province, with the exception of mountainous northwest region, where complex terrain makes spiral flights unsafe.¹ In April 2008, the monthly mean daily average temperature in Zhengzhou was relatively stable at 16.0 ± 5.0 C° (data from www.wunderground.com), so we assumed the sulfur emissions from coal burning for electricity generation, domestic heating, and cooking did not change dramatically during the campaign. Therefore, we selected the region covered by the research flights (33.0° to 35.5°N, 112.5° to 115.5°E, hereafter named the campaign area) and calculated the campaign average SO₂ profile from the airborne measurements (Figure 3). The integral of SO₂ with respect to altitude gives a mean SO₂ column content of 0.73 Dobson Unit (DU, 1 DU = 2.69 × 10¹⁶ molecules/cm²). The majority of SO₂ was found in the PBL and in the lower atmosphere with an effective scale height of SO₂ of ~800 m, from surface up to ~1800 m. The mean profile also showed substantial amounts of SO₂ aloft in the FT, where atmospheric SO₂ has a longer lifetime, and is more likely to be converted to sulfate aerosols. The relatively strong winds in the FT transport sulfurous pollutants over greater distances, and SO₂ in the FT has a greater impact on large-scale air quality and climate.

¹Auxiliary materials are available in the HTML. doi:10.1029/2011JD016473.

Table 1. Summary of Research Flights^a

Date	Spiral				Descent			
	Altitude (m)	SO ₂ Conc. (ppbv)			Altitude (m)	SO ₂ Conc. (ppbv)		
		Mean	Stdev	Median		Mean	Stdev	Median
4/4/2008	1000	4.67	0.29	4.67	500	7.16	0.87	7.02
	1500	3.74	0.27	3.84	1000	5.14	3.38	3.13
	2000	2.71	0.34	2.63	1500	1.31	0.33	1.25
	2500	1.72	0.26	1.65	2000	1.00	0.06	1.01
	3000	1.79	0.32	1.81				
	3500	1.23	0.22	1.21				
	4000	0.87	0.06	0.89				
4/5/2008	1000	4.81	0.32	4.93	500	9.48	4.18	8.51
	1500	6.08	0.75	5.94	1000	2.07	1.42	1.29
	2000	7.31	0.13	7.34	1500	0.97	0.52	1.24
	2500	5.96	1.06	6.26	2000	0.20	0.06	0.21
	3000	2.29	0.83	2.00				
	3500	1.50	0.07	1.49				
	4000	1.08	0.16	1.07				
4/15/2008	1000	3.00	0.12	2.95	500	4.99	1.86	6.00
	1500	1.86	0.79	1.58	1000	0.88	0.72	0.52
	2000	1.07	0.04	1.08	1500	0.51	0.05	0.50
	2500	0.91	0.07	0.91	2000	0.54	0.03	0.53
	3000	0.93	0.18	0.92				
	3500	1.28	0.09	1.24				
	4000	1.34	0.05	1.35				
4/16/2008	1500	0.29	0.12	0.31	500	3.62	1.52	4.35
	2000	0.18	0.05	0.19	1000	0.42	0.05	0.41
	2500	0.23	0.03	0.23	1500	0.16	0.23	0.11
	3000	0.21	0.10	0.22	2000	0.15	0.08	0.19
	3500	0.32	0.09	0.35				
4/18/2008	1500	-0.06	0.06	-0.04	500	3.30	0.35	3.40
	2000	-0.08	0.04	-0.07	1000	1.38	1.08	1.63
	2500	-0.11	0.08	-0.10	1500	0.00	0.03	-0.01
	3000	0.04	0.11	0.09	2000	0.03	0.05	0.02
	3500	0.25	0.13	0.19				
4/20/2008	3000	0.98	0.05	0.98	500	4.14	1.71	4.65
	3500	1.08	0.17	1.12	1000	0.29	0.15	0.22
	4000	1.98	0.44	1.79	1500	0.22	0.02	0.21
	2000	0.70	0.31	0.58				
4/22/2008	1500	-0.14	0.02	-0.14	500	3.82	0.10	3.83
	2000	-0.11	0.07	-0.06	1000	1.04	1.13	0.41
	2500	-0.14	0.09	-0.19	1500	0.35	0.09	0.38
	3000	-0.09	0.09	-0.04	2000	0.38	0.07	0.36
	3500	-0.03	0.04	-0.03				
	4000	-0.05	0.05	-0.04				

^aNegative values are beyond the detection limit of 43C SO₂ analyzer. Spirals were conducted over Changyuan (April 4 and 5), Shangcai (April 15), Suiping (33.15°N, 113.95°E, April 16), Yexian (April 18 and 22), and Weishi (34.41°N, 114.17°E, April 20). Descents were all conducted over CGO airport. Conc., concentration.

[16] Figure 3 also shows all the SO₂ measurements from the campaign. The distribution of SO₂ measurements exhibits large variability, especially between 1000 and 3000 m, which is above the typical PBL height during spring in central China. During the campaign, we frequently observed isolated SO₂ plumes in the FT, and the statistics of SO₂ concentrations aloft were greatly influenced by these plumes. All of the research flights were conducted under calm and stable weather conditions without strong convection, so the FT SO₂ plumes were likely related to up wind or large-scale vertical transport. Similar characteristics were observed in Mid-Atlantic region of the U.S. [Hains *et al.*, 2008; Taubman

et al., 2006]. In Table 2, we summarize the FT SO₂ plumes observed during the campaign. To study the transport processes, we calculated 72-h back-trajectories using the NOAA Hybrid Single Particle Lagrangian Integrated Trajectory Model (HYSPLIT, <http://www.arl.noaa.gov/ready/hysplit4.html>), with the Global Data Assimilation System (GDAS) meteorological fields. Time and height of the observed SO₂ plumes were utilized as release time and release height (plume height \pm 500 m). For example, Plume 1 demonstrated a stagnant case with air circulating within a radius of 400 km. The deep polluted dry air mass indicated that the lower atmosphere was well mixed. The back-trajectory calculation for plumes 2 and 5 did not demonstrate an upward lifting

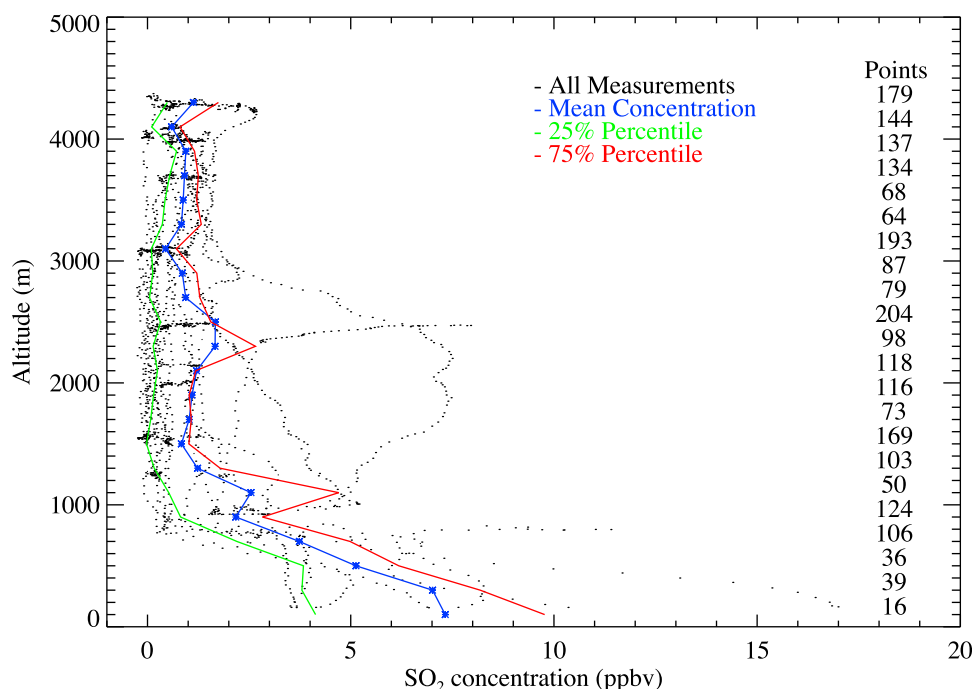


Figure 3. In situ measurements and the mean SO_2 profile. The mean profile is calculated by averaging every 200 m from the surface to 4500 m. Green and red lines indicate the 25th and 75th percentiles. The numbers on the right are the number of valid SO_2 data points within the 200 m layer. The concentration of SO_2 decreases from the surface to ~ 1800 m with an effective scale height of 800 m, but strata of SO_2 were frequently observed aloft.

motion, implying the sub-grid convection could be important. Figure 4 presents the case study of Plume 3, which existed at a high elevation with high RH value. The back-trajectory suggested a case of long-range transport with what appeared to be isentropic lifting from southern China. The air mass was lifted from the surface to 4200 m and transported around 1500 km in 72 h. Based on GPS data, this plume had a minimum size of 22 km in width and 1000 m in depth. With a mean concentration of 2 ppbv, the total mass of atmospheric SO_2 in the plume was estimated to be at least 1.5 tons. The substantial amount of SO_2 in FT shows the importance of studying large-scale lifting to understand inter-continental transport of pollutants from East Asia.

4. Evaluation of OMI SO_2 PBL Products

[17] OMI SO_2 products proved useful for research flight planning during the campaign, and in this section we quantitatively evaluate the products. To estimate the accuracies and characterize the limitations of these OMI SO_2 retrievals (both archived operational OMISO2 PBL product and new off-line research ISF product), independent coincident column

measurements were needed. The ceiling of in situ measurements conducted during the aircraft campaign was ~ 4500 m, well into the free troposphere. These vertical SO_2 profiles showed that during this campaign, significant amount of ambient SO_2 was found within the PBL (< 1 km). Therefore the integration of aircraft vertical profiles can be used to validate OMI satellite retrievals.

[18] We compared the in situ SO_2 vertical columns with co-located archived OMISO2 PBL values and with the research ISF retrievals using prescribed SO_2 shapes with center of mass altitude (CMAs) similar to the measured in situ profiles over the aircraft spiral locations and their surrounding areas. Following the comparison approach described earlier [Krotkov *et al.*, 2008], the average values of the nearest eight pixels in 30 km radius of spiral locations were compared with the corresponding vertically integrated in situ SO_2 columns. The uncertainties of the satellite measurements were estimated as the largest of the OMI average background noise (i.e., 0.62 DU for 8 pixel mean error for the PBL product [Krotkov *et al.*, 2008] and standard deviations of the eight nearest pixels). Note that this error estimate approach yields an upper limit,

Table 2. Summary of SO_2 Plumes Observed in the FT^a

Number	Date	Time (UTC)	Location	Conc. (ppbv)	Altitude (m)	Size (km)	RH (%)
1	4/15/2008	6:05–6:13	33.85N°, 114.50E°	2.0~8.0	2500~4000	30	30
2	4/16/2008	7:00–7:07	34.36N°, 114.31E°	1.3	3700	26	75
3	4/20/2008	3:34–3:42	35.26N°, 114.70E°	2.6	4200	22	90
4	4/20/2008	4:00–4:13	34.54N°, 115.20E°	2.2	4300	18	100
5	4/22/2008	6:53–7:03	33.93N°, 113.11E°	1.6	3700	22	20

^aConc., concentration; RH, relative humidity.

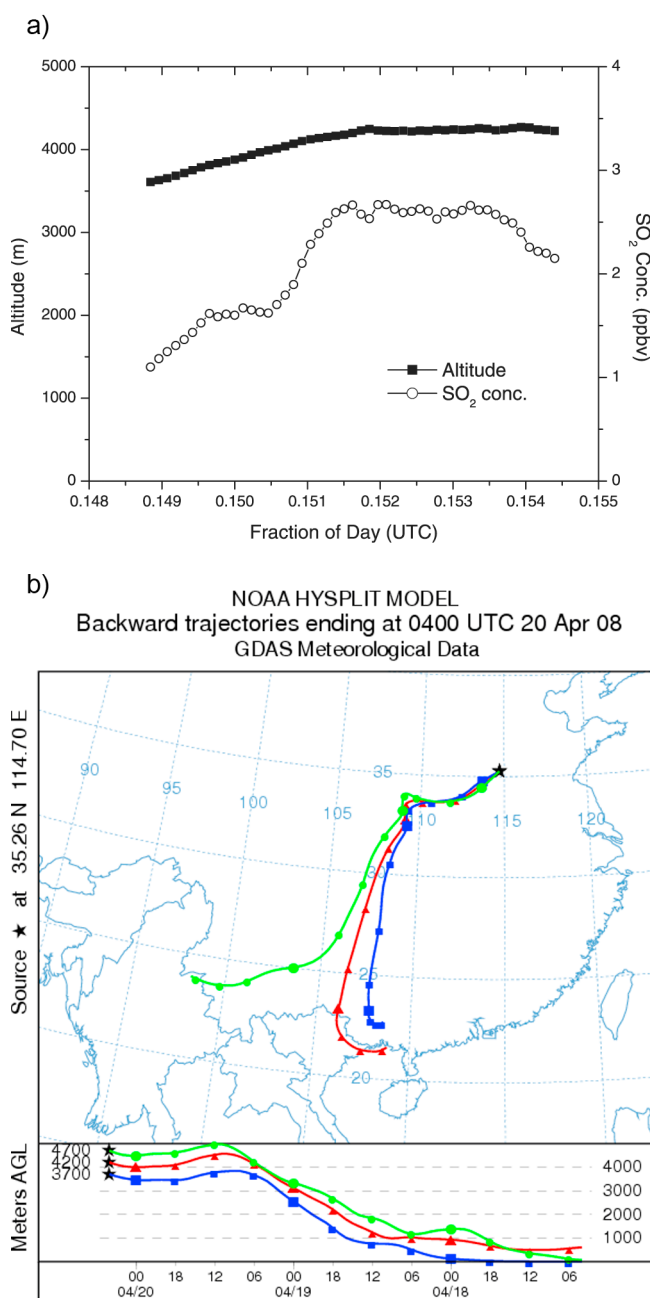


Figure 4. SO₂ plumes in FT and the HYSPLIT back trajectory. (a) Ambient SO₂ concentration versus aircraft altitude; (b) 72-h back trajectory (ending at 0400 UTC, 04/20/2008) of Plume 3. These high altitude plumes affect the OMI retrieval and can be transported relatively long distance.

because it includes the natural variability of SO₂ spatial distribution as part of the error.

[19] To estimate the error of total column integrated from the in situ concentrations, we need to account for the fact that during the campaign over Henan, many spirals were restricted to altitudes above 1000 m, therefore concentrations below this altitude (down to the ground) were not simultaneously measured. The column amount missed by the aircraft measurements below ~1000 m usually accounts for 10–30% of the

total SO₂ PBL column [Lee *et al.*, 2009], and it makes the largest contribution to the error budget of aircraft measured total columns. To compensate for these missing columns, we used the in situ SO₂ measurements obtained during the aircraft landings at the airport, whose location is different from those of the spirals. In doing so, we assumed that the partial column SO₂ amount in the lowest part of the atmosphere is homogeneous, and therefore is the same as the mean value observed during descent on the same day. Under this assumption the uncertainty of the total vertical SO₂ column is estimated to be half of the added partial column, as the distance between the descent and spiral is less than 200 km. A certain degree of correlation of PBL columns between the two locations is expected.

[20] We compared SO₂ columns estimated using in situ measurements and OMISO2 PBL products as the Ordinary Least Squares (OLS) linear regression (auxiliary material Figure S2). The OLS slope (0.16) was low, indicating that OMI greatly underestimated the SO₂ PBL column contents. The OMISO2 PBL products have variable bias, which need to be removed empirically [Fioletov *et al.*, 2011]. Here we added 0.4 DU to all OMISO2 PBL data to make them physically meaningful, and compared the results with in situ measurements (Figure 5a). The comparison showed a strong correlation ($r = 0.84$), higher than that obtained from validation studies over North America, but the slope (0.54) was still lower than the previously reported slope found in the comparisons of improved OMI products during INTEX-A and INTEX-B campaign [Lee *et al.*, 2009]. In that study, OMI PBL data were post-corrected applying local air mass factor (AMF) calculated using monthly SO₂ profile shapes and aerosol climatology from the global Goddard Earth Observing System (GEOS-CHEM) chemical transport model. The correction resulted in typically reduced SO₂ values over oceans, including INTEX-A and INTEX-B regions. However, over China the local AMFs [Lee *et al.*, 2009] were close to the operational value ~0.4 [Krotkov *et al.*, 2008]. Therefore, no local AMF correction was applied in this study. The OMI PBL products underestimated the tropospheric SO₂ column by ~50% likely due to (1) systematic negative biases in OMISO2 PBL values when the satellite field of views were cloud contaminated; (2) reduced satellite measurement sensitivity to SO₂ in the lowest levels due to the presence of aerosols, and (3) spatial averaging of local SO₂ plumes over large OMI pixel size. Low visibility (high aerosol concentrations) conditions were common during our research flights. Visibility observations (available at www.wunderground.com) at the CGO airport at 9 A.M. (local time) from March 28 to April 26 2008 showed most of the flight days with visibility less than 5 km. The OMI instrument has lower sensitivity to the SO₂ close to the surface compared to those in the upper atmosphere. The presence of aerosols above or co-located with the SO₂ layer would further reduce this sensitivity, leading to an SO₂ underestimate, since aerosol effects are not accounted for in the operational PBL products. During the EAST-AIRE campaign, the local AMFs could be reduced to ~0.2, half of the operational AMF (0.4), due to dust aerosols [Krotkov *et al.*, 2008], implying the OMISO2 PBL products could be doubled to compensate the underestimate of AMFs, while no correction of AMFs was conducted in this study.

[21] To reduce these random errors, we averaged all OMI PBL pixel values over the campaign area for April 2008.

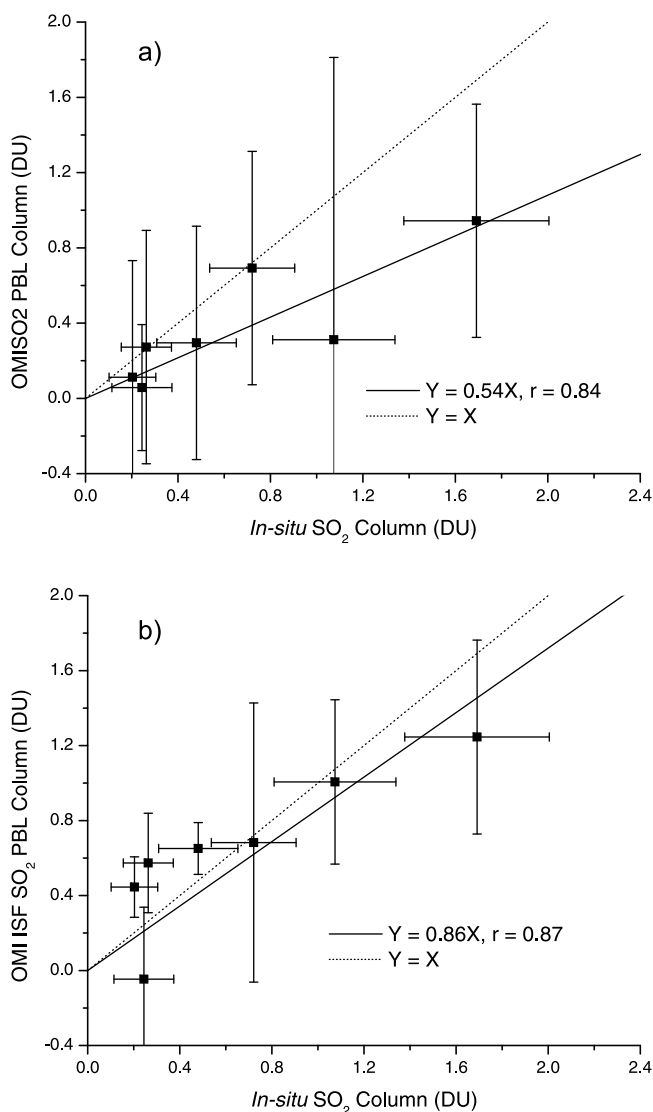


Figure 5. Evaluation of in situ measurements with (a) modified OMISO2 PBL (+0.4 DU) and (b) ISF SO₂ Column Content. The dotted line represents the $Y = X$ line. X and Y error bars describe the uncertainties of aircraft observation and OMI PBL column respectively. Solid line presents the OLS linear regression passing through zero. Both retrievals capture the average column content, but the ISF algorithm shows substantially better fit to individual daily observations.

The resulted regional monthly mean ($\pm\sigma$) SO₂ column was 0.63 (± 0.26) DU, close to 0.73 DU obtained from averaging all aircraft measurements. This suggests that averaged over a month and a large region, the OMI PBL data can capture the PBL SO₂ column contents better than them for individual days.

[22] We also compared the integrated in situ data with off-line ISF retrievals (Figure 5b). The ISF algorithm demonstrated similar correlation ($r = 0.87$), but less noise and better evaluation (slope = 0.86) of PBL SO₂ columns, compared with the operational OMISO2 products. Systematic bias was not observed, though our comparisons indicate that current ISF retrievals still have low bias with respect to the airborne

observations over central China. The underestimate could be caused by the similar reasons discussed above, so the algorithm needs to be improved in this respect possibly through incorporation of tropospheric aerosols information in future.

5. Numerical Simulations of SO₂ Over Central China

5.1. WRF-CMAQ Model Setup

[23] In this study, we used the WRF V3.1 model [National Center for Atmospheric Research, 2010] to generate meteorological fields for the CMAQ model. Figure 6 shows the two WRF domains in a Lambert projection. The coarse domain (30 km grid cells) covered the central and eastern part of China, where most of the population and industry were located, and the nested domain (10 km grid cells) focused on the campaign region. The U.S. Geological Survey (USGS) 24-category data were used to determine the terrain and land use. We used the NCEP Final Operational Model Global Tropospheric Analyses (FNL) (<http://dss.ucar.edu/datasets/ds083.2>) as initial and boundary conditions. The NCEP FNL are on $1^\circ \times 1^\circ$ grids with 26 vertical levels from 1000 to 10 hPa with a time frame of 6 h. The major physics options used in the WRF simulation included Thompson microphysics scheme [Thompson, 2006], YSU boundary layer scheme [Hong and Lim, 2006], Kain-Fritsch (new Eta) cumulus scheme [Kain, 2004], Monin-Obukhov surface-layer scheme [Foken, 2006] and Noah land-surface scheme [Ek et al., 2003]. The model was run with 35 vertical layers from the surface to 50 hPa with the first 12 layers in the PBL, and re-initialized every 5 d to reduce simulation errors. MCIP V3.5 was applied to process the WRF outputs to create CMAQ-ready meteorology inputs [Byun and Ching, 1999].

[24] We used the CMAQ version 4.6 (released in September 2006) [Byun and Schere, 2006] to conduct a 45-d simulation

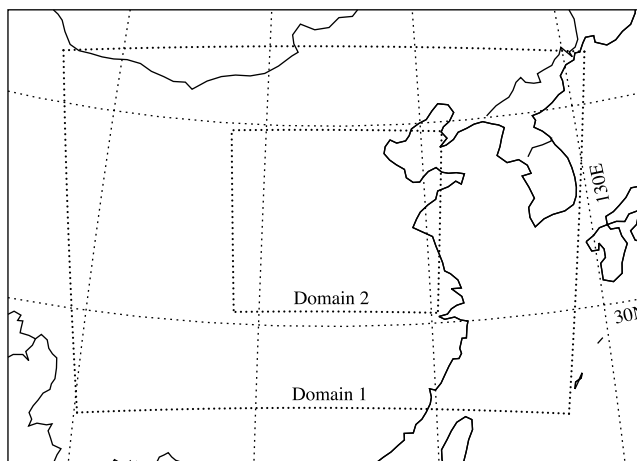


Figure 6. Domains of the WRF simulation. Both the coarse and nested domains are centered at Zhengzhou City (34.8°N , 113.7°E). The coarse domain has 97×69 grids and 30 km resolution, and the nested domain has 117×102 grids and 10 km resolution. The CMAQ domains are 2 grid cells smaller on each side of the WRF domains to eliminate the lateral effect.

from 03/13/2008 to 04/26/2008, with the first 15 days as spin-up. CMAQ was run with a coarse and nested domain with the same horizontal and vertical resolutions as the WRF simulation. Chemical initial and boundary conditions for the coarse domain were obtained from the Regional Acid Deposition Model, version 2 (RADM2) concentration profiles [Community Modeling and Analysis System, 2007; Stockwell *et al.*, 1990]. The SAPRC99 scheme and the 4th generation aerosols scheme (AE4) were selected as the gas-chemistry mechanism and aerosol modules respectively. The Regional Acid Deposition Model (RADM) based cloud processor with the asymmetric convection model (ACM) was applied for the aqueous/cloud chemical mechanism. The CMAQ output files included hourly 3-D fields of gaseous and aerosol species concentrations.

5.2. The Emission Inventory

[25] We selected the NASA INTEX-B emission inventory (available at <http://mic.greensource.cn/intex-b2006>) for the CMAQ simulations, although there is evidence that emissions decreased between 2006 and 2008 [Witte *et al.*, 2009]. This latest emission inventory of East Asia was based on the year 2006 with estimates of all major anthropogenic sources [Zhang *et al.*, 2009], including major pollutants (SO_2 , NO_x , CO, PM_{10} , $\text{PM}_{2.5}$, BC, and OC) and 30 lumped VOC species for SAPRC-99 chemical mechanism with a resolution of $0.5^\circ \times 0.5^\circ$. Compared with EPA's National Emission Inventory (NEI) database, INTEX-B only contained area emission sources, and lacked point sources, mobile sources and other geographic information. Therefore, we could not use the Sparse Matrix Operator Kernel Emission (SMOKE) model to create the 3-D emission input data for CMAQ, and had to create our own emission input data through the following steps. First, we incorporated the 2008 NH_3 emission prediction from the REAS program (available at <http://www.jamstec.go.jp/frsgc/research/d4/emission.htm>) as supplement. Second, INTEX-B had each pollutant calculated individually for four sectors: Electricity Generation, Industry, Residential Emission and Transportation, and we allocated them into two groups: the Electricity Generation and Others. Since stack parameters such as plume exit velocity and plume exit temperature were not available, Electricity Generation emissions were located 200 m above the surface as an approximation of average stack height and plume rise. Third, we speciated the emission data of NO_x and $\text{PM}_{2.5}$ into NO_2 , NO, sulfate and nitrate aerosols to accommodate the SAPRC99 mechanism. Last, we averaged the yearly emission values into hourly values arithmetically, and allocated them into the CMAQ grid cells through bilinear interpolation, to create a 3-D emission input data with constant values for all chemical species.

[26] The INTEX-B inventory estimated total emission of SO_2 for China was 31.0 Tg per year with $\pm 12\%$ reported uncertainty, and the arithmetic mean daily SO_2 emission was 84.9 kT, which was close to 84.8 kT and 78.9 kT from the arithmetic mean from March and April emissions respectively [Zhang *et al.*, 2009]. These values implied that the seasonality of SO_2 emissions was negligible during spring in China. We ignored the diurnal cycle of emissions by assuming constant emission rates since there was no available information on diurnal variation. For demonstration, we presented the resulting SO_2 emission maps

(auxiliary material Figure S3), which correspond well to the location of cities, populations and industrial centers in China such as YRD. This spatial accuracy was crucial to the CMAQ simulations. The manipulation of INTEX-B emission inventory created CMAQ emission input files without seasonal and diurnal variations. The effects of using 2006 INTEX – B emissions on CMAQ simulations for 2008 will be discussed in section 7.

5.3. Modification of the CMAQ System

[27] Version 3.5 of MCIP was used to ingest the WRF output and create meteorological input files for the CMAQ model. We modified MCIP to write out the percentage of each WRF grid cell that is urban, and the new urban fraction variable was used to calculate vertical diffusion in CMAQ [Castellanos, 2009]. The SO_2 dry deposition velocity was calculated in the MCIP program. In the default MCIP setting, the mean SO_2 dry deposition velocity ($\pm\sigma$) was 0.58 ± 0.07 cm/s over the campaign area, which is substantially higher than $0.2 \sim 0.4$ cm/s measured over northern China [Sorimachi *et al.*, 2003; Sorimachi and Sakamoto, 2007] and other areas [Clarke *et al.*, 1997]. To decrease the simulated dry deposition rate, we set the mesophyll resistance of SO_2 from 0 (default value) to 8000 s/m [Pfanzer *et al.*, 1987] in the MCIP model. Similar modification successfully decreased the CO dry deposition velocity from ~ 0.4 cm/s to ~ 0.1 cm/s [Castellanos *et al.*, 2011].

[28] The CMAQ model was modified to facilitate our analysis of the sulfur budget. To estimate the export of S (sulfur) from China, the CMAQ code was modified to output the flux of each species due to horizontal advection entering and leaving the domain through changing the advection scheme from the Yamartino (HYAMO) scheme to the new Piecewise Parabolic Method (HPPM) scheme [Loughner, 2011; Loughner *et al.*, 2011]. This allowed pollutant fluxes, deposition, and emissions to be studied collectively, and we applied these results to study the S budget and export in section 6.3. To investigate influences on SO_2 chemistry from these modifications, we conducted three sensitivity runs: (1) default mesophyll resistance (MR), and HYAMO advection scheme; (2) default MR and HPPM scheme; and (3) updated MR and HPPM scheme. They are named NoMR_HYAMO, NoMR_HPPM, and MR_HPPM respectively.

[29] To isolate effects of modifying SO_2 mesophyll resistance, the difference between results from NoMR_HPPM and MR_HPPM was calculated. We selected data over the campaign area (mostly grassy plain with good vegetation coverage), on days with calm weather and no precipitation to minimize the effects of SO_2 wet deposition. The monthly average dry deposition velocity ($\pm\sigma$) of the MR_HPPM run was 0.24 ± 0.06 cm/s, $\sim 60\%$ lower than the NoMR_HPPM run with the value of 0.58 ± 0.07 cm/s. We also investigated the SO_2 dry deposition flux, calculated in the CMAQ model. The monthly mean value ($\pm\sigma$) decreased from 0.093 ± 0.039 $\mu\text{g}/\text{m}^2$ s with NoMR_HPPM to 0.045 ± 0.031 $\mu\text{g}/\text{m}^2$ s with MR_HPPM, a 52% reduction. The MR_HPPM value is around 50% less than a lab experiment conducted in northern China, but the SO_2 dry deposition process is influenced by other factors such as soil type and meteorological conditions [Sorimachi and Sakamoto, 2007]. These results show that a better parameterization of SO_2 dry deposition is needed for future development of the CMAQ model.

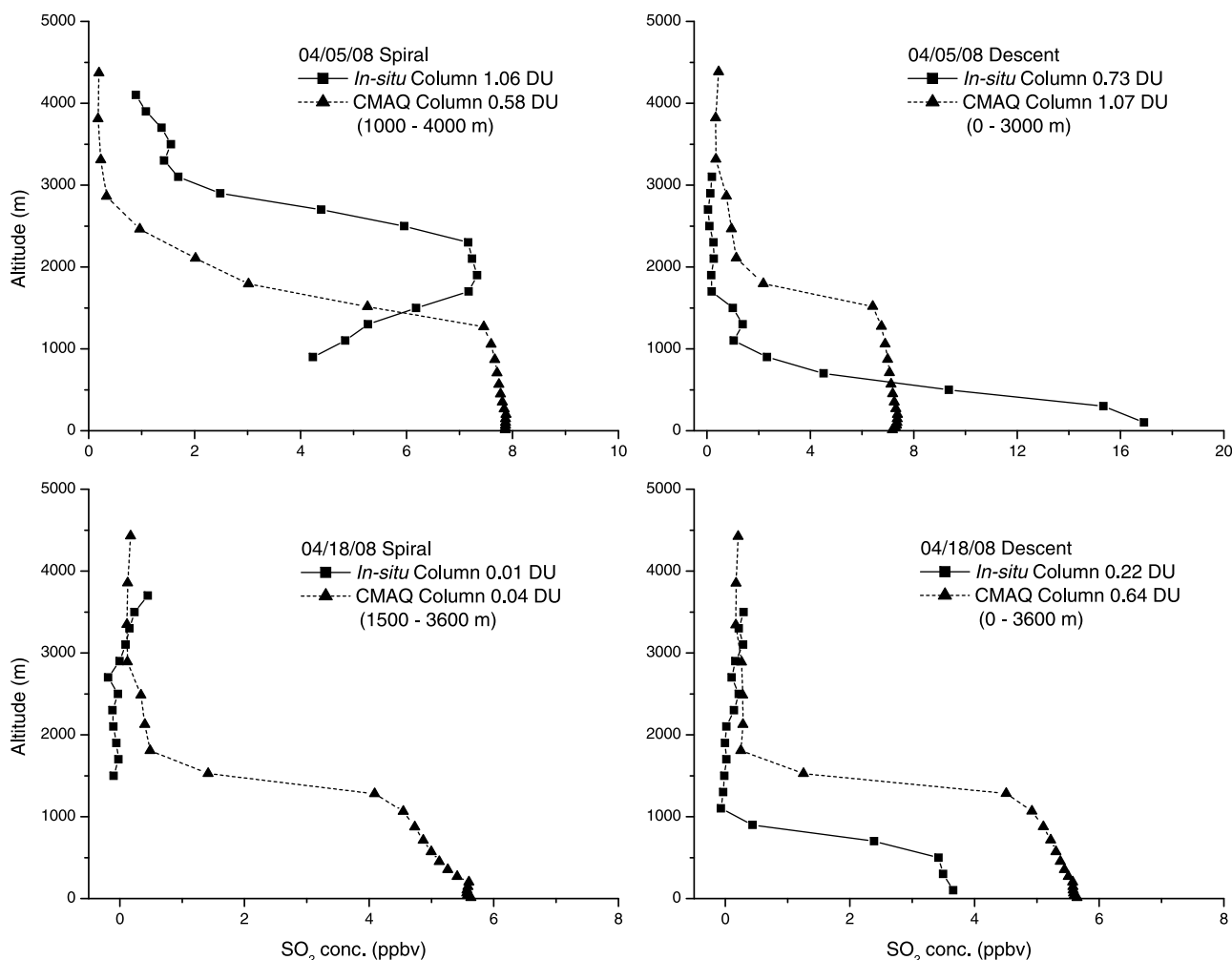


Figure 7. Comparison of aircraft measurements and CMAQ simulations. The in situ measurements are obtained by averaging the aircraft SO_2 profiles every 200 m from surface to 4500 m. The CMAQ SO_2 column contents are calculated by integrating the SO_2 at the same altitudes as aircraft measurements. The model cannot fully resolve the subgrid scale processes responsible for SO_2 plumes aloft.

Hereafter in the following sections, we use results from MR_HPPM run and discuss the details of the three sensitivity runs in section 6.1.

6. Results of CMAQ Simulation and Discussion

6.1. Evaluation of CMAQ Simulations

[30] We compared two days' flight data with the CMAQ results, and found that the SO_2 profiles were not precisely simulated especially within the PBL (Figure 7). We also checked CMAQ simulations for the FT SO_2 plumes discussed in Table 2, and the model did not reproduce these plumes well. This implies that CMAQ (with 10 km resolution) had difficulty reproducing the vertical SO_2 altitude profiles at specific times and locations. Other studies have shown that CMAQ has similar problems with vertical profiles of trace gases over the eastern U.S. [Castellanos *et al.*, 2011; Lee *et al.*, 2011]. These issues were probably due to sub-grid scale convective lifting, and the model resolution of

10 km was apparently inadequate to simulate the vertical mixing [Loughner *et al.*, 2011].

[31] Other sources of uncertainty include the precision of winds. Due to limited resource, we did not use the Four-Dimensional Data Assimilation (FDDA) in WRF simulations. Without FDDA, wind errors were expected resulting in uncertainty of CMAQ simulations [Otte, 2008]. SO_2 emissions from power plants were estimated at 200 m AGL, however these plumes could rise to several hundred meters under certain weather conditions. Therefore, we focused on comparisons of SO_2 column contents of each research flight to the corresponding SO_2 columns from CMAQ simulations in Figure 8. The CMAQ simulations had a moderately strong correlation ($r = 0.62$) with the integrated aircraft measurements, with a slope of 1.33. This indicated that CMAQ provided a reasonable representation of the spatial/temporal variation of total SO_2 loading over the campaign area and $\sim 30\%$ overestimate was observed.

[32] Figure 9 compares CMAQ monthly mean SO_2 profile over the campaign region, with the mean aircraft campaign

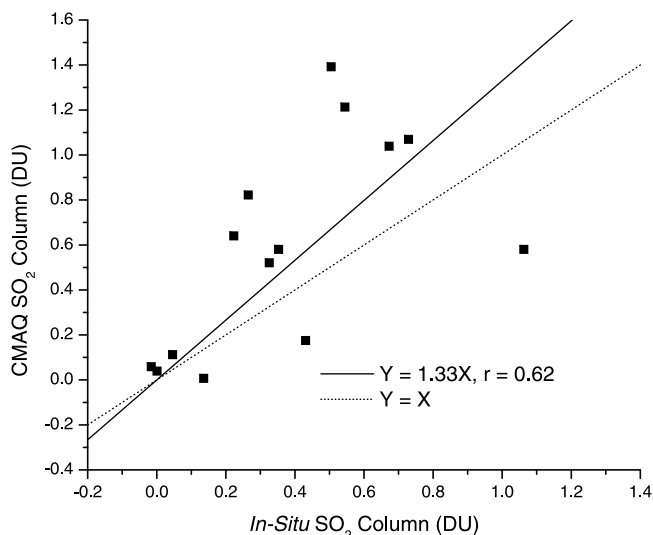


Figure 8. Evaluation of in situ and CMAQ SO₂ column contents. The CMAQ SO₂ column was calculated over corresponding altitude of research flights. The dotted line represents the $Y = X$ line. The solid line presents the OSL linear regression, and there were 7 flights and 14 profiles giving 6–13 degrees of freedom.

profile. The monthly mean MR_HPPM profile underestimated the ambient SO₂ near the surface, overestimated the SO₂ between 600 and 2200 m, and underestimated the SO₂ above 2500 m. The total SO₂ column was ~38% higher than the value obtained during the aircraft campaign. All the three sensitivity runs over predicted the SO₂ columns. Based on differences of the NoMR_HPPM and MR_HPPM cases, it was confirmed that decrease of the SO₂ dry deposition increased the ambient SO₂ column content. Due to little SO₂ emission in the upwind western China, the comparison between the NoMR_HYAMO

and NoMR_HPPM cases implied that the HPPM advection scheme transported less SO₂ out of the domain. The default CMAQ set up (NoMR_HYAMO case) demonstrated the best estimate of total SO₂ column content, while the modified case (MR_HPPM) had the best estimate of SO₂ concentration near the surface. Besides uncertainties in meteorological and emission data, the underestimate/overestimate within/above the PBL implied that the CMAQ model might mix the lower atmosphere too fast to transport the pollutants out of the PBL, also observed in the eastern U.S. [Castellanos *et al.*, 2011].

[33] To summarize, the CMAQ simulations demonstrated reasonable accuracy (~30% overestimate) in reproducing the SO₂ column content observed during the research flights, but the SO₂ model profiles had substantial differences with respect to the measured SO₂ vertical distributions. More accurate model representation of pollutant vertical distribution will require better parameterization of vertical transport and mixing in future. The comparison of monthly mean SO₂ profiles from sensitivity runs showed that the CMAQ model overestimated the SO₂ column content by 25 ~ 40% from difference sensitivity runs. The discrepancies are probably caused by the decrease from the 2006 emission inventory used in this CMAQ simulation. The recent decreasing trend in Chinese SO₂ pollution has been observed in number of studies [Li *et al.*, 2010b; Lu *et al.*, 2010; Witte *et al.*, 2009] and attributed to wide installation of Flue Gas Desulfurization (FGD) equipment on coal burning power plants.

6.2. SO₂ Chemistry and Lifetime

[34] To investigate the conversion of SO₂ to other sulfur-compounds such as sulfate aerosols, we estimated lifetime of tropospheric SO₂. A simple box model was applied to the nested domain (area with $\sim 1.25 \times 10^6$ km²), and the SO₂ lifetime was calculated as $\tau_{SO_2} = \frac{\text{Loading}}{\text{Emission}}$. The average SO₂ emission was 4.3×10^{-3} mol/km² s based on the INTEX-B emission inventory. The campaign mean SO₂ loading from

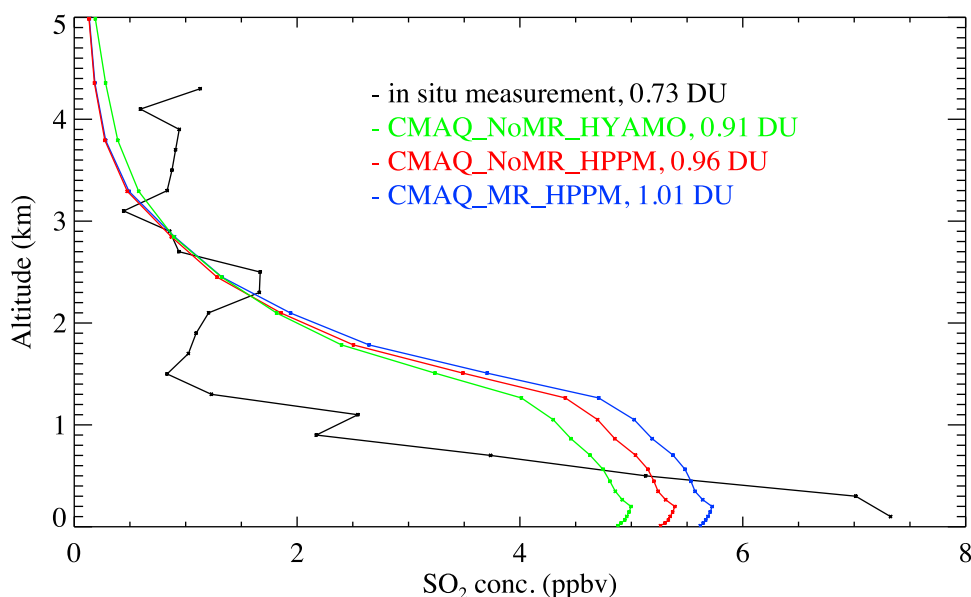


Figure 9. Comparison of monthly mean profiles of in situ measurements and CMAQ sensitivity runs. The SO₂ vertical column amount is the integral from the surface to 5000 m.

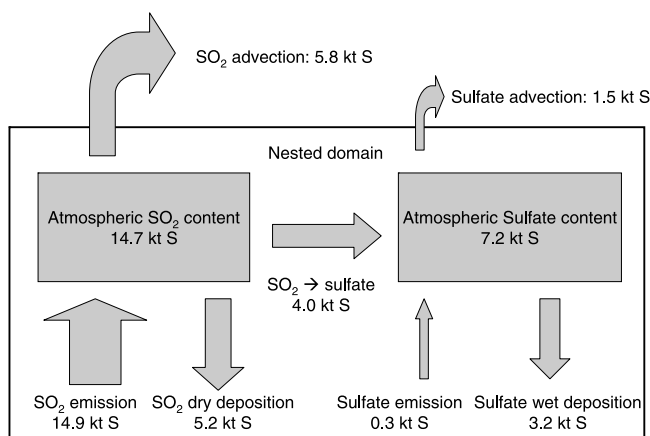


Figure 10. Budget of sulfur-compounds over the central China. The units for reservoirs are kT = (1 kT = 10^6 kg), or kT/d for fluxes. All the data are the average daily value from the month-long simulations.

the aircraft campaign was 326 mol/km^2 , and the SO_2 lifetime with respect to all losses from the domain (deposition, chemical transformation, and advection) was 21.0 h. The lifetime was shorter than the result from a global model simulation [Lee *et al.*, 2011]. In summer over the Mid-Atlantic, the observed lifetime for chemical removal and deposition was 19 ± 7 h [Hains, 2007]. April in China is cooler and drier than summer over the Mid-Atlantic resulting in low photochemical reactivity, and a longer SO_2 lifetime is expected. The shortcoming of this approach was that the ambient SO_2 was assumed being emitted within the box model region. The size of nested domain was only $\sim 1000 \times 1000$ km, so an air mass with the typical wind speed of 10 m/s would move through it within one day. Therefore, substantial transport of sulfur-compounds in and/or out of the domain was expected.

[35] Modification of the CMAQ advection scheme provided the ability to calculate the advection of pollutants through the boundaries; therefore we can investigate the budget of sulfur-compounds (SO_2 and sulfate aerosols). To simplify the computation, we described all sulfur-compounds in units of kT S. The reacted SO_2 amount, calculated as $\text{SO}_2(\text{reactive}) = \text{Emission} - \text{Deposition} - \text{Advection}$, assumed that the SO_2 oxidation product was 100% sulfate aerosols, i.e., 1 mol SO_2 is equivalent to 1 mol of sulfate. Figure 10 presents the monthly mean budget of sulfur-compounds of the nested domain, in units of kT/day. The daily SO_2 emission was 14.9 kT S and the monthly average SO_2 content in the domain was 14.7 kT S. The major sinks of SO_2 include daily dry deposition of 5.2 kT S and advection of 5.8 kT S out of the domain. The average rate of oxidation of SO_2 was assumed as 4.0 kT S/d, which generated the same amount of S in sulfate aerosols. The direct sulfate input from the emission inventory was small, 0.3 kT S. The discrepancy of sulfate budget (*sources* – *sinks*) is 0.5 kT S, accounting for less than 3% of the total daily S emission (14.9 kT S), which could be caused by (1) assuming the 100% conversion from SO_2 to sulfate aerosols and ignoring the pathways to form other sulfur-compounds such as sulfuric acid vapor (H_2SO_4); and (2) neglecting minor

deposition processes such as SO_2 wet deposition and sulfate dry deposition. We re-calculated the lifetime of SO_2 as $\tau_{\text{SO}_2} = \frac{\text{Loading}}{\text{Emission} - \text{Export}}$. Based on Figure 10, the total amount of exported SO_2 was 5.8 kT/d, which accounts for $\sim 39\%$ of the total emitted SO_2 . Including error analyses, the CMAQ simulated SO_2 budget and lifetime was computed for each day of the campaign, and the average lifetime ($\pm\sigma$) was 38 ± 7 h. Due to significant advection, the oxidation rate was substantially decreased and the SO_2 lifetime is consistent with results from global model simulations [Lee *et al.*, 2011], and the case study in northern China with a SO_2 lifetime of ~ 2 d [Li *et al.*, 2010a].

6.3. Estimated Sulfur Transport and Error Analysis

[36] We further investigated the sinks and transport of sulfur-compounds. The daily total deposition (wet + dry) was 8.4 kT S, accounting for 55% of the total sulfur emission. This demonstrated the importance of controlling sulfur emissions for mitigating the soil and water acidification in central China [Larssen *et al.*, 2006]. Daily, 7.3 kT S were transported out of the domain, and the monthly mean ($\pm\sigma$) S of daily export was $48 \pm 7\%$ of the total sulfur emission.

[37] Our estimate of atmospheric sulfur export from central China is subject to random and systematic errors. The random uncertainty can be estimated from the standard deviation of daily sulfur export, 7%. A systematic bias is incurred if the month was atypical with respect to pollutant exports. April 2008 was observed as a generally wet month, with more precipitation than normal, 54 mm in April 2008 compared with 43 mm for long-term monthly average precipitation (data from www.wunderground.com). The WRF-CMAQ model also reproduced the wet month, therefore our approach using CMAQ simulations would overestimate the average sulfur wet deposition and underestimate export. We assumed conservatively the overestimation as half of the mean sulfate wet deposition: 1.6 kT S/d, or 10.5% of total S emissions (14.9 kT/d). Finally, errors in the simulated vertical distribution of SO_2 (Figure 9) affected the horizontal flux. We calculated the difference of average SO_2 concentration between in situ measurements and CMAQ as +0.5 ppbv, -2.0 ppbv and +0.5 ppbv for layers 3000 ~ 4500 m, 500 ~ 2000 m, and surface to 500 m respectively. The wind speeds for these layers were estimated at 15 m/s, 8 m/s and 5 m/s respectively, based on statistics of zonal mean flow. The SO_2 export was proportional to the product of SO_2 concentration and wind speed. So the CMAQ model had biases of +1.0 kT S, -3.0 kT S and +0.3 kT S for these three layers, which resulted in a net overestimate of 1.7 kT S in export, i.e., +11% of the total sulfur-compound emission. Adding these three uncertainties ($\pm 7\%$ and $\pm 11\%$) in quadrature provided an estimate of the total uncertainty for our estimate of S export. We concluded that 48% ($\pm 13\%$) of the S emitted into the atmosphere over central China was exported. The uncertainties were not Gaussian distributions, but we estimated the confidence interval as 90% for the range of 35 ~ 61%.

[38] The nested domain is located in central China, and there are limited sulfur emissions in the upwind region of less developed western China. The study of pollutant transport demonstrated that most of the exported sulfur-compounds were transported through the northern and eastern boundary to the western Pacific coast (auxiliary material Figures S4a–S4d).

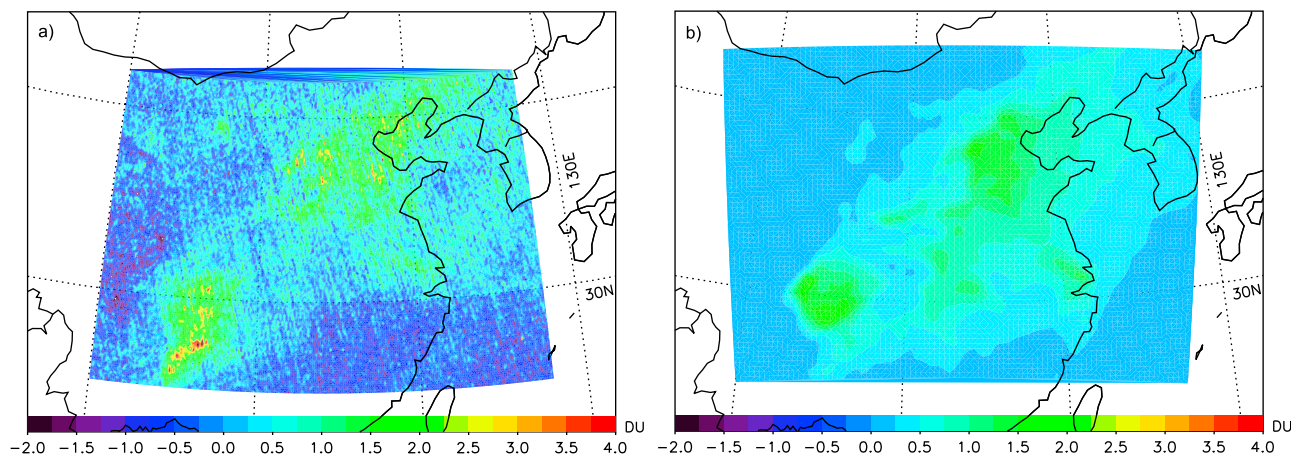


Figure 11. Monthly average SO_2 column maps of the CMAQ simulations and OMI PBL products. (a) OMI SO_2 PBL column, 42 kT in $4.5 \times 10^6 \text{ km}^2$; white color describe the location of clouds; (b) CMAQ SO_2 column map, 54 kT in $4.6 \times 10^6 \text{ km}^2$.

Prior studies on S budgets through airborne measurements [Koike *et al.*, 2003] and model simulations [Tan *et al.*, 2002] also reported that around half of the sulfur-compounds were exported to the ocean. Quantifying long-range transport is crucial for understanding the regional/global air quality and climate change due to emissions from East Asia.

6.4. Estimate of SO_2 Emissions in Central and Eastern China

[39] In section 3, we calculated the monthly mean OMI SO_2 column content over the campaign region as 0.63 ± 0.26 DU, which agrees with the observed aircraft average SO_2 column. CMAQ overestimated the monthly mean SO_2 column over the campaign region with a column content of 1.01 DU. The CMAQ high bias could be due to SO_2 being transported from nearby regions into the small campaign region. Because of small size, the OMI instrument had only ~ 150 pixels per day within the campaign region. To reduce the noise and eliminate the influence of SO_2 transport, we selected CMAQ results of coarse domain (Figure 6) to study the total SO_2 burden over central and eastern China. The coarse domain ($\sim 4.6 \times 10^6 \text{ km}^2$) covered most of the industrialized regions in China, and emitted ~ 25 Tg SO_2/year , $\sim 80\%$ of the total SO_2 emission in China [Zhang *et al.*, 2009]. We sampled CMAQ and OMISO2 PBL columns over the region with OMI reactive cloud fraction less than 0.3 (hereafter named cloud-free condition), in order to reduce cloud effects on the satellite retrievals.

[40] A daily comparison was conducted on the CMAQ SO_2 and OMISO2 columns for 04/05/2008 (auxiliary material Figures S5a and S5b). The CMAQ simulations captured the large-scale SO_2 plumes in the northeast and southeast of China, but missed the plume in the northwest. We found the daily OMI SO_2 map had large variability due to both uneven coverage (sparse data on the east and west side of the domain) and instrument noise (negative value up to -2.0 DU). The CMAQ model overestimated the SO_2 burden by 10% compared with the OMISO2 product for 04/05/2008. To reduce the uncertainties of daily data, we presented the monthly average SO_2 column map for both data sets (Figure 11). The

CMAQ model captured the hot spots of SO_2 well over land, but missed the plumes off the coast. Column differences (OMI – CMAQ) were calculated resulting in a mean difference of -0.16 DU, and the histogram and probability density was analyzed (auxiliary material Figure S6) indicating a negative bias. So the CMAQ simulations systematically overestimated the SO_2 column by ~ 0.16 DU compared with OMISO2 PBL data. The monthly mean SO_2 loadings ($\pm\sigma$) were 54 ± 22 kT and 42 ± 26 kT for CMAQ simulations and OMISO2 PBL products respectively. Because both the OMISO2 products and CMAQ simulations were sampled under cloud-free conditions using OMI radiative cloud fraction, these absolute low bias was expected to daily OMISO2 and CMAQ SO_2 loadings. The monthly mean cloud-free fraction ($\pm\sigma$) was $56 \pm 15\%$. The same approach of sulfur export error analysis was adopted here, i.e., underestimate as half of SO_2 loading filtered out. The systematic low bias was estimated as $+21$ kT and $+16$ kT for CMAQ simulations and OMISO2 PBL products respectively, therefore the mean SO_2 loadings with all uncertainties were 54 (55 \sim 97) kT and 42 (37 \sim 89) kT. The result revealed that CMAQ simulations overestimated OMI SO_2 column contents by $\sim 30\%$, consistent with the relative change in SO_2 emissions in China recently [Lu *et al.*, 2010].

[41] As a summary, CMAQ simulations with the INTEX-B emission inventory demonstrated reasonable performance in describing the intensity and spatial distribution of sulfur-compound emissions in China. Both statistical analyses and total SO_2 loading computation indicated that CMAQ overestimated the SO_2 column contents compared with OMI products, suggesting this might be due to the use of 2006 emission inventory; our results are consistent with reported decreasing trends of sulfur emission from 2006 to 2008 in China [Lu *et al.*, 2010; Witte *et al.*, 2009].

7. Discussion and Conclusions

[42] Using a combination of in situ and remotely sensed measurement along with numerical simulation, we were able to evaluate the SO_2 concentration and chemistry over central China – one of the most densely populated regions in the

world. The CMAQ simulations served as a powerful tool to investigate tropospheric sulfur pollutants. Among the most important sources of uncertainties in the numerical simulations was the emission inventory, which was developed for the year 2006. Our campaign was conducted in 2008, and from 2006 to 2008, especially in order to improve the air quality for the 2008 Beijing Olympics, sulfur emissions in China were decreased through stricter regulations on the usage of high sulfur coal and installations of FGD equipment in power plants. The decreasing trend has been observed [Okuda et al., 2011; Witte et al., 2009], so the INTEX-B emission inventory probably has a high bias, resulting in overestimated anthropogenic SO₂ emissions in the CMAQ simulations for spring 2008. A comparison with campaign SO₂ column contents demonstrated that CMAQ overestimated the tropospheric SO₂ columns over Henan by ~30%, and a similar overprediction, also ~30%, was obtained through comparing monthly CMAQ and OMI SO₂ column contents over central and eastern China. These results are consistent with the reduction of sulfur emissions observed in China between years 2006 and 2008.

[43] During the campaign, the aircraft instrument frequently observed SO₂ plumes in the FT, important for satellite retrieval and long-range transport. We found the SO₂ concentrations had high temporal and spatial variability during spring in China. Comparisons of in situ measurements, the operational OMISO2 PBL products revealed good agreement, and the new ISF algorithm demonstrated better performance and will be employed operationally in the future. The CMAQ model didn't capture the SO₂ vertical distribution well, probably due to inadequate model resolution for computing vertical mixing. But the CMAQ simulations agreed with the mean aircraft measurements, with a ~30% overestimation. With a modified CMAQ advection scheme, we investigated the budget and transport of SO₂ and sulfate. The lifetime of SO₂ with respect to all reactions and removal from the atmosphere was 38 ± 7 h, relatively long for spring. Due to the slow removal and strong winds in spring, ~50% (35 ~ 61%) of the total S emitted into the atmosphere in central and eastern China was transported out of the domain. Further research in East Asia will help to improve our knowledge on the effects on regional air quality and large-scale climate downstream.

[44] **Acknowledgments.** We thank Qiang Zhang at Tsinghua University for the discussion on the application of INTEX-B emission inventory. We thank R. J. Salawitch for helpful comments. This work was supported by NASA (NNX08AH71G), DOE (DESC0007171) and UMD.

References

- Albrecht, B. A. (1989), Aerosols, cloud microphysics, and fractional cloudiness, *Science*, *245*(4923), 1227–1230, doi:10.1126/science.245.4923.1227.
- Berglen, T. F., T. K. Berntsen, I. S. A. Isaksen, and J. K. Sundet (2004), A global model of the coupled sulfur/oxidant chemistry in the troposphere: The sulfur cycle, *J. Geophys. Res.*, *109*, D19310, doi:10.1029/2003JD003948.
- Byun, D. W., and J. E. Ching (1999), Meteorology-Chemistry Interface Processor (MCIP) for Models-3 Community Multiscale Air Quality (CMAQ) modeling system, in *Science Algorithm of the EPA Models-3 Community Multi-scale Air Quality (CMAQ) Modeling System*, EPA/600/R-99/030, pp. 12.1–12.87, U.S. EPA, Research Triangle Park, N. C.
- Byun, D., and K. L. Schere (2006), Review of the governing equations, computational algorithms, and other components of the models-3 Community Multiscale Air Quality (CMAQ) modeling system, *Appl. Mech. Rev.*, *59*(1–6), 51–77.
- Calvert, J. G., et al. (1978), Mechanism of homogeneous oxidation of sulfur dioxide in troposphere, *Atmos. Environ.*, *12*(1–3), 197–226, doi:10.1016/0004-6981(78)90201-9.
- Castellanos, P. (2009), Analysis of air quality with numerical simulations (CMAQ), and observations of trace gases, PhD dissertation, Univ. of Md., College Park.
- Castellanos, P., L. T. Marufu, B. G. Doddridge, B. F. Taubman, J. J. Schwab, J. C. Hains, S. H. Ehrman, and R. R. Dickerson (2011), Ozone, oxides of nitrogen, and carbon monoxide during pollution events over the eastern United States: An evaluation of emissions and vertical mixing, *J. Geophys. Res.*, *116*, D16307, doi:10.1029/2010JD014540.
- CESY (2005), *Energy Statistical Yearbook in 2005*, China Stat. Press, Beijing.
- Chin, M., D. J. Jacob, G. M. Gardner, M. S. Foreman-Fowler, P. A. Spiro, and D. L. Savoie (1996), A global three-dimensional model of tropospheric sulfate, *J. Geophys. Res.*, *101*(D13), 18,667–18,690, doi:10.1029/96JD01221.
- Clarke, J. F., et al. (1997), Dry deposition calculations for the clean air status and trends network, *Atmos. Environ.*, *31*(21), 3667–3678, doi:10.1016/S1352-2310(97)00141-6.
- Community Modeling and Analysis System (2007), CMAQ v4.6 operational guidance document, report, Univ. of N. C. at Chapel Hill, Chapel Hill.
- Costabile, F., et al. (2006), A preliminary assessment of major air pollutants in the city of Suzhou, China, *Atmos. Environ.*, *40*(33), 6380–6395, doi:10.1016/j.atmosenv.2006.05.056.
- Cox, R. A., and S. A. Penkett (1971), Photo-oxidation of atmospheric SO₂, *Nature*, *229*(5285), 486–488, doi:10.1038/229486a0.
- Dickerson, R. R., et al. (2007), Aircraft observations of dust and pollutants over northeast China: Insight into the meteorological mechanisms of transport, *J. Geophys. Res.*, *112*, D24S90, doi:10.1029/2007JD008999.
- Dunlea, E. J., et al. (2009), Evolution of Asian aerosols during transpacific transport in INTEX-B, *Atmos. Chem. Phys.*, *9*(19), 7257–7287, doi:10.5194/acp-9-7257-2009.
- Eggleston, A. E. J., and R. A. Cox (1978), Homogeneous oxidation of sulfur compounds in atmosphere, *Atmos. Environ.*, *12*(1–3), 227–230, doi:10.1016/0004-6981(78)90202-0.
- Ek, M. B., K. E. Mitchell, Y. Lin, E. Rogers, P. Grunmann, V. Koren, G. Gayno, and J. D. Tarpley (2003), Implementation of Noah land surface model advances in the National Centers for Environmental Prediction operational mesoscale Eta model, *J. Geophys. Res.*, *108*(D22), 8851, doi:10.1029/2002JD003296.
- Fioletov, V. E., et al. (2011), Estimation of SO₂ emissions using OMI retrievals, *Geophys. Res. Lett.*, *38*, L21811, doi:10.1029/2011GL049402.
- Foken, T. (2006), 50 years of the Monin-Obukhov similarity theory, *Boundary Layer Meteorol.*, *119*(3), 431–447, doi:10.1007/s10546-006-9048-6.
- Geng, F. H., et al. (2009), Aircraft measurements of O₃, NO_x, CO, VOCs, and SO₂ in the Yangtze River Delta region, *Atmos. Environ.*, *43*(3), 584–593, doi:10.1016/j.atmosenv.2008.10.021.
- Hains, J. C. (2007), A chemical climatology of lower tropospheric trace gases and aerosols over the mid-Atlantic region, PhD dissertation, Univ. of Md., College Park.
- Hains, J. C., et al. (2008), Origins of chemical pollution derived from Mid-Atlantic aircraft profiles using a clustering technique, *Atmos. Environ.*, *42*(8), 1727–1741, doi:10.1016/j.atmosenv.2007.11.052.
- Hand, J. L., and W. C. Malm (2007), Review of aerosol mass scattering efficiencies from ground-based measurements since 1990, *J. Geophys. Res.*, *112*, D16203, doi:10.1029/2007JD008484.
- Haywood, J., and O. Boucher (2000), Estimates of the direct and indirect radiative forcing due to tropospheric aerosols: A review, *Rev. Geophys.*, *38*(4), 513–543, doi:10.1029/1999RG000078.
- He, K. B., et al. (2002), Urban air pollution in China: Current status, characteristics, and progress, *Annu. Rev. Energy Environ.*, *27*, 397–431, doi:10.1146/annurev.energy.27.122001.083421.
- Hong, S.-Y., and J.-O. Lim (2006), The WRF single-moment 6-class microphysics scheme (WSM6), *J. Korean Meteorol. Soc.*, *42*, 129–151.
- Hu, H., et al. (2010), Air pollution and control in different areas of China, *Crit. Rev. Environ. Sci. Technol.*, *40*(6), 452–518, doi:10.1080/10643380802451946.
- Igarashi, Y., et al. (2006), Seasonal variations in SO₂ plume transport over Japan: Observations at the summit of Mt. Fuji from winter to summer, *Atmos. Environ.*, *40*(36), 7018–7033, doi:10.1016/j.atmosenv.2006.06.017.
- Intergovernmental Panel on Climate Change (2007), *Climate Change 2007: The Physical Science Basis, Contribution of Working Group I to the Fourth Assessment Report (AR4) of the Intergovernmental Panel on Climate Change*, 996 pp., Cambridge Univ. Press, Cambridge, U. K.
- Kain, J. S. (2004), The Kain-Fritsch convective parameterization: An update, *J. Appl. Meteorol.*, *43*(1), 170–181, doi:10.1175/1520-0450(2004)043<0170:TKCPAU>2.0.CO;2.

- Kan, H. D., et al. (2010), Short-term association between sulfur dioxide and daily mortality: The Public Health and Air Pollution in Asia (PAPA) study, *Environ. Res.*, *110*(3), 258–264, doi:10.1016/j.envres.2010.01.006.
- Kim, B. G., et al. (2001), Transport of SO₂ and aerosol over the Yellow sea, *Atmos. Environ.*, *35*(4), 727–737, doi:10.1016/S1352-2310(00)00344-7.
- Koike, M., et al. (2003), Export of anthropogenic reactive nitrogen and sulfur compounds from the East Asia region in spring, *J. Geophys. Res.*, *108*(D20), 8789, doi:10.1029/2002JD003284.
- Krotkov, N. A., et al. (2006), Band residual difference algorithm for retrieval of SO₂ from the aura Ozone Monitoring Instrument (OMI), *IEEE Trans. Geosci. Remote Sens.*, *44*(5), 1259–1266, doi:10.1109/TGRS.2005.861932.
- Krotkov, N. A., et al. (2008), Validation of SO₂ retrievals from the Ozone Monitoring Instrument over NE China, *J. Geophys. Res.*, *113*, D16S40, doi:10.1029/2007JD008818.
- Larssen, T., et al. (2006), Acid rain in China, *Environ. Sci. Technol.*, *40*(2), 418–425, doi:10.1021/es0626133.
- Lee, C., R. V. Martin, A. van Donkelaar, G. O'Byrne, N. Krotkov, A. Richter, L. G. Huey, and J. S. Holloway (2009), Retrieval of vertical columns of sulfur dioxide from SCIAMACHY and OMI: Air mass factor algorithm development, validation, and error analysis, *J. Geophys. Res.*, *114*, D22303, doi:10.1029/2009JD012123.
- Lee, C., R. V. Martin, A. van Donkelaar, H. Lee, R. R. Dickerson, J. C. Hains, N. Krotkov, A. Richter, K. Vinnikov, and J. J. Schwab (2011), SO₂ emissions and lifetimes: Estimates from inverse modeling using in situ and global, space-based (SCIAMACHY and OMI) observations, *J. Geophys. Res.*, *116*, D06304, doi:10.1029/2010JD014758.
- Li, C., L. T. Marufu, R. R. Dickerson, Z. Li, T. Wen, Y. Wang, P. Wang, H. Chen, and J. W. Stehr (2007), In situ measurements of trace gases and aerosol optical properties at a rural site in northern China during East Asian Study of Tropospheric Aerosols: An International Regional Experiment 2005, *J. Geophys. Res.*, *112*, D22S04, doi:10.1029/2006JD007592.
- Li, C., N. A. Krotkov, R. R. Dickerson, Z. Li, K. Yang, and M. Chin (2010a), Transport and evolution of a pollution plume from northern China: A satellite-based case study, *J. Geophys. Res.*, *115*, D00K03, doi:10.1029/2009JD012245.
- Li, C., Q. Zhang, N. A. Krotkov, D. G. Streets, K. He, S.-C. Tsay, and J. F. Gleason (2010b), Recent large reduction in sulfur dioxide emissions from Chinese power plants observed by the Ozone Monitoring Instrument, *Geophys. Res. Lett.*, *37*, L08807, doi:10.1029/2010GL042594.
- Li, Z. Q., et al. (2007), Preface to special section on east Asian studies of tropospheric aerosols: An international regional experiment (EAST-AIRE), *J. Geophys. Res.*, *112*, D22S00, doi:10.1029/2007JD008853.
- Li, Z. Q., et al. (2011), East Asian Studies of Tropospheric Aerosols and their Impact on Regional Climate (EAST-AIRC): An overview, *J. Geophys. Res.*, *116*, D00K34, doi:10.1029/2010JD015257.
- Lin, M. Y., et al. (2008), Long-range transport of acidifying substances in East Asia - Part I - Model evaluation and sensitivity studies, *Atmos. Environ.*, *42*(24), 5939–5955, doi:10.1016/j.atmosenv.2008.04.008.
- Liu, X. H., et al. (2010), Understanding of regional air pollution over China using CMAQ, part I, performance evaluation and seasonal variation, *Atmos. Environ.*, *44*(20), 2415–2426, doi:10.1016/j.atmosenv.2010.03.035.
- Loughner, C. (2011), Impacts of fair-weather cumulus clouds, bay breezes, and landuse on urban air quality and climate, PhD dissertation, Univ. of Md., College Park.
- Loughner, C. P., et al. (2011), Impact of fair-weather cumulus clouds and the Chesapeake Bay breeze on pollutant transport and transformation, *Atmos. Environ.*, *45*(24), 4060–4072, doi:10.1016/j.atmosenv.2011.04.003.
- Lu, Z., et al. (2010), Sulfur dioxide emissions in China and sulfur trends in East Asia since 2000, *Atmos. Chem. Phys.*, *10*(13), 6311–6331, doi:10.5194/acp-10-6311-2010.
- Luke, W. T. (1997), Evaluation of a commercial pulsed fluorescence detector for the measurement of low-level SO₂ concentrations during the gas-phase sulfur intercomparison experiment, *J. Geophys. Res.*, *102*(D13), 16,255–16,265, doi:10.1029/96JD03347.
- Meng, Z. Y., et al. (2010), Ambient sulfur dioxide, nitrogen dioxide, and ammonia at ten background and rural sites in China during 2007–2008, *Atmos. Environ.*, *44*(21–22), 2625–2631, doi:10.1016/j.atmosenv.2010.04.008.
- National Center for Atmospheric Research (2010), *Weather Research and Forecasting, ARW Version 3 Modeling System's User Guide*, Mesoscale and Microscale Meteorol. Div., Boulder, Colo.
- Okuda, T., et al. (2011), The impact of the pollution control measures for the 2008 Beijing Olympic Games on the chemical composition of aerosols, *Atmos. Environ.*, *45*(16), 2789–2794, doi:10.1016/j.atmosenv.2011.01.053.
- Otte, T. L. (2008), The impact of nudging in the meteorological model for retrospective air quality simulations. Part I: Evaluation against national observation networks, *J. Appl. Meteorol. Climatol.*, *47*(7), 1853–1867, doi:10.1175/2007JAMC1790.1.
- Pfan, H., et al. (1987), Mesophyll resistances to SO₂ fluxes into leaves, *Plant Physiol.*, *85*(4), 922–927, doi:10.1104/pp.85.4.922.
- Prospero, J. M., D. L. Savoie, and R. Arimoto (2003), Long-term record of nss-sulfate and nitrate in aerosols on Midway Island, 1981–2000: Evidence of increased (now decreasing?) anthropogenic emissions from Asia, *J. Geophys. Res.*, *108*(D1), 4019, doi:10.1029/2001JD001524.
- Schlesinger, R. B., and F. Cassee (2003), Atmospheric secondary inorganic particulate matter: The toxicological perspective as a basis for health effects risk assessment, *Inhal. Toxicol.*, *15*(3), 197–235, doi:10.1080/08958370304503.
- Shannon, J. D., and D. L. Sisterson (1992), Estimation of S and NO_x-N deposition budgets for the United States and Canada, *Water Air Soil Pollut.*, *63*(3–4), 211–235, doi:10.1007/BF00475491.
- Singh, H. B., et al. (2009), Chemistry and transport of pollution over the Gulf of Mexico and the Pacific: Spring 2006 INTEX-B campaign overview and first results, *Atmos. Chem. Phys.*, *9*(7), 2301–2318, doi:10.5194/acp-9-2301-2009.
- Sorimachi, A., and K. Sakamoto (2007), Laboratory measurement of the dry deposition of sulfur dioxide onto northern Chinese soil samples, *Atmos. Environ.*, *41*(13), 2862–2869, doi:10.1016/j.atmosenv.2006.10.025.
- Sorimachi, A., et al. (2003), Measurements of sulfur dioxide and ozone dry deposition over short vegetation in northern China—A preliminary study, *Atmos. Environ.*, *37*(22), 3157–3166, doi:10.1016/S1352-2310(03)00180-8.
- Stier, P., et al. (2007), Aerosol absorption and radiative forcing, *Atmos. Chem. Phys.*, *7*(19), 5237–5261, doi:10.5194/acp-7-5237-2007.
- Stockwell, W. R., P. Middleton, J. S. Chang, and X. Tang (1990), The second generation Regional Acid Deposition Model chemical mechanism for regional air-quality modeling, *J. Geophys. Res.*, *95*(D10), 16,343–16,367, doi:10.1029/JD095iD10p16343.
- Sun, Y., et al. (2009), Measurement of the vertical profile of atmospheric SO₂ during the heating period in Beijing on days of high air pollution, *Atmos. Environ.*, *43*(2), 468–472, doi:10.1016/j.atmosenv.2008.09.057.
- Tan, Q., Y. Huang, and W. L. Chameides (2002), Budget and export of anthropogenic SO₂ from East Asia during continental outflow conditions, *J. Geophys. Res.*, *107*(D13), 4167, doi:10.1029/2001JD000769.
- Taubman, B. F., J. C. Hains, A. M. Thompson, L. T. Marufu, B. G. Doddridge, J. W. Stehr, C. A. Piety, and R. R. Dickerson (2006), Aircraft vertical profiles of trace gas and aerosol pollution over the mid-Atlantic United States: Statistics and meteorological cluster analysis, *J. Geophys. Res.*, *111*, D10S07, doi:10.1029/2005JD006196.
- Thompson, G. E., et al. (2006), A new bulk microphysical parameterization for WRF (& MM5), paper presented at Seventh Weather Research and Forecasting User's Workshop, NCAR, Boulder, Colo.
- Tu, F. H., D. C. Thornton, A. R. Bandy, G. R. Carmichael, Y. Tang, K. L. Thornhill, G. W. Sachse, and D. R. Blake (2004), Long-range transport of sulfur dioxide in the central Pacific, *J. Geophys. Res.*, *109*, D15S08, doi:10.1029/2003JD004309.
- Twomey, S. (1977), Influence of pollution on shortwave albedo of clouds, *J. Atmos. Sci.*, *34*(7), 1149–1152, doi:10.1175/1520-0469(1977)034<1149:TIOPOT>2.0.CO;2.
- U.S. Environmental Protection Agency (2004), Air quality criteria for particulate matter (final report, Oct 2004), *EPA 600/P-99/002aF-bF*, Washington, D. C.
- van Donkelaar, A., et al. (2008), Analysis of aircraft and satellite measurements from the Intercontinental Chemical Transport Experiment (INTEX-B) to quantify long-range transport of East Asian sulfur to Canada, *Atmos. Chem. Phys.*, *8*(11), 2999–3014, doi:10.5194/acp-8-2999-2008.
- Wang, L. T., et al. (2010a), Assessment of air quality benefits from national air pollution control policies in China. Part I: Background, emission scenarios and evaluation of meteorological predictions, *Atmos. Environ.*, *44*(28), 3442–3448, doi:10.1016/j.atmosenv.2010.05.051.
- Wang, L. T., et al. (2010b), Assessment of air quality benefits from national air pollution control policies in China. Part II: Evaluation of air quality predictions and air quality benefits assessment, *Atmos. Environ.*, *44*(28), 3449–3457, doi:10.1016/j.atmosenv.2010.05.058.
- Wang, W., et al. (2008), Aircraft measurements of gaseous pollutants and particulate matter over Pearl River Delta in China, *Atmos. Environ.*, *42*(25), 6187–6202, doi:10.1016/j.atmosenv.2008.06.001.
- Wesely, M. L., and B. B. Hicks (2000), A review of the current status of knowledge on dry deposition, *Atmos. Environ.*, *34*(12–14), 2261–2282, doi:10.1016/S1352-2310(99)00467-7.
- Witte, J. C., M. R. Schoeberl, A. R. Douglass, J. F. Gleason, N. A. Krotkov, J. C. Gille, K. E. Pickering, and N. Livesey (2009), Satellite observations of changes in air quality during the 2008 Beijing Olympics and Paralympics, *Geophys. Res. Lett.*, *36*, L17803, doi:10.1029/2009GL039236.
- Xue, L. K., et al. (2010), Aircraft measurements of the vertical distribution of sulfur dioxide and aerosol scattering coefficient in China, *Atmos. Environ.*, *44*(2), 278–282, doi:10.1016/j.atmosenv.2009.10.026.

- Yang, K., N. A. Krotkov, A. J. Krueger, S. A. Carn, P. K. Bhartia, and P. F. Levelt (2009a), Improving retrieval of volcanic sulfur dioxide from back-scattered UV satellite observations, *Geophys. Res. Lett.*, *36*, L03102, doi:10.1029/2008GL036036.
- Yang, K., X. Liu, N. A. Krotkov, A. J. Krueger, and S. A. Carn (2009b), Estimating the altitude of volcanic sulfur dioxide plumes from space borne hyper-spectral UV measurements, *Geophys. Res. Lett.*, *36*, L10803, doi:10.1029/2009GL038025.
- Yang, K., X. Liu, P. K. Bhartia, N. A. Krotkov, S. A. Carn, E. J. Hughes, A. J. Krueger, R. J. D. Spurr, and S. G. Trahan (2010), Direct retrieval of sulfur dioxide amount and altitude from spaceborne hyperspectral UV measurements: Theory and application, *J. Geophys. Res.*, *115*, D00L09, doi:10.1029/2010JD013982.
- Zhang, Q., et al. (2009), Asian emissions in 2006 for the NASA INTEX-B mission, *Atmos. Chem. Phys.*, *9*(14), 5131–5153, doi:10.5194/acp-9-5131-2009.
- Zhang, Y. H., et al. (2008), Regional Integrated Experiments on Air Quality over Pearl River Delta 2004 (PRIDE-PRD2004), Overview, *Atmos. Environ.*, *42*(25), 6157–6173, doi:10.1016/j.atmosenv.2008.03.025.
-
- X. Bao and G. Zhao, Henan Meteorological Bureau, Zhengzhou 450003, China.
- R. Dickerson and H. He, Department of Atmospheric and Oceanic Science, University of Maryland, College Park, MD 20742, USA. (russ@atmos.umd.edu)
- N. A. Krotkov and K. Yang, NASA Goddard Space Flight Center, Greenbelt, MD 20771, USA.
- C. Li, Z. Li, and C. P. Loughner, Earth System Science Interdisciplinary Center, University of Maryland, College Park, MD 20740, USA.
- L. Wang and Y. Zheng, Nanjing University of Information Science and Technology, Nanjing 210044, China.